Differ Equ Dyn Syst (January–July 2019) 27(1–3):57–74
https://doi.org/10.1007/s12591-017-0373-7

ORIGINAL RESEARCH

Singularly Perturbed Vector Field Method (SPVF) Applied to Combustion of Monodisperse Fuel Spray

OPhir Nave[1]

Published online: 29 June 2017

Abstract In this paper we present the concept of singularly perturbed vector field (SPVF) method, and its application to thermal explosion of diesel spray combustion. Given a system of governing equations, which consist of hidden Multi-scale variables, the SPVF method transfer and decompose such system to fast and slow singularly perturbed subsystems. The resulting subsystem enables us to understand better the complex system, and to simplify the calculations. Later powerful analytical, numerical and asymptotic methods [e.g method of integral (invariant) manifold, the homotopy analysis method etc.] can be applied to each subsystem. In this paper, we compare the results obtained by the methods of integral invariant manifold and SPVF as applied to the spray droplets combustion model.

Keywords Polydisperse spray · Model reduction · Asymptotic analysis · Multi-scale systems

Contents

✉ OPhir Nave
naveof@cs.bgu.ac.il

[1] Department of Mathematics, Jerusalem College of Technology, Jerusalem, Israel

Nomenclature:

A	Pre-exponential factor $(1/s)$
B	Universal gas constant $(Jkmol^{-1}K^{-1})$
C	Molar concentration $(kmolm^{-3})$
c	Specific heat capacity $(Jkg^{-1}K^{-1})$
E	Activation energy $(Jkmol^{-1})$
L	Liquid evaporation energy (i.e., latent heat of evaporation, Enthalpy of evaporation) (Jkg^{-1})
m	Different size of droplets' radii
n	Number of droplets per unit volume (m^{-3})
Q	Combustion energy (Jkg^{-1})
R	Radius of droplet (m)
T	Temperature (K)
t	Time (s)

Subscripts:

d	Liquid fuel droplets
f	Combustible gas component of the mixture
g	Gas mixture
p	Under constant pressure
0	Initial state

Introduction

Mathematical models that related to various engineering application, are usually described by a large set of complex equations (differential equations). For the purpose of numerical, analytical and qualitative analysis, it is often desirable to reduce the system to a smaller system with a comparatively small loss of accuracy. Generally, a large set of differential equations describing a complex realistic phenomenon has a number of essentially different time scales (i.e. rates of change) which correspond to sub-processes. Given such systems, there is a great difficulty in revealing the hidden hierarchy, the implicit multi-time scale of the original systems which govern the equations and, hence one cannot apply asymptotic methods. On one hand, discovering the hierarchical structure of systems requires considerable complicated numerical treatments, but on the other hand, this known hierarchical structure allows applying a number of asymptotic approaches for the analysis of their behavior. There are several asymptotic methods and numerical tools that can be applied to multi-scale systems. For example the method of integral invariant manifold (MIM), that has been applied to thermal ignition of diesel spray [1–4], the iteration method of Fraser and Roussel [5–8], the computational singular perturbation (CSP) method [9,10], geometric singular perturbation theory [11–13], and the intrinsic low dimensional method (ILDM) which is a numerical method [14–18]. The ILDM-method successfully locates slow manifolds of considered system, but also has a number of principal problems. The main constraints of the ILDM-method are as follows: the algorithm cannot be applied on domains of phase space, where the RHS leading eigenvalues of the Jacobian matrix of the considered system are complex. In this case the ILDM method does not produce any decomposition of the original system or pro-

duces an incorrect decomposition. Even in the case of an explicitly known decomposition, the ILDM cannot treat some zones on the phase plane such as the turning zones (manifolds), i.e. zones where critical changes in the system behavior occur, the numerical algorithm of the method produces additional non relevant solutions to the system dynamics (ghost manifolds). A modification of the ILDM method is the transposition intrinsic low dimensional method (TILDM). TILDM is based on the geometrical approach for the hierarchical systems of ordinary differential equations. Although all these methods as well as most reduction methods have been applied successfully to many engineering problems, models of reacting flows etc., they have some principle restrictions and drawback some of which have been mentioned above. The main problem of these methods is the lack of tools for hierarchy identification of the system, i.e., fast and slow subsystem. Researches in the field of combustion theory suggested a new method called global quasi linearization (GQL), and singular perturbed vector field (SPVF) to solve the above problems [19–26]. The main idea of this method is to transfer the original system of the governing equations with the hidden hierarchy (hidden multi-scale structure) to its explicit form as a singularly perturbed system (SPS). When one finds this transformation from a hidden hierarchy model into a model with standard SPS, the analysis of the original system can be treated by the very powerful machinery of the standard SPS theory for model reduction and decomposition, as we mention above. The global information about the decomposition of the model is very useful and able to provide the qualitative structure of the slow and fast manifold [22]. This paper deals with the SPVF method as applied to thermal explosion of fuel spray.

Preliminaries to the SPVF Method

Given a large and complex scientific model with nonlinear governing equations, the aim of this research is to reduce the number of equations and to discover the hierarchy of the dynamical variables of the system, i.e., to decompose the system into subsystems with fast and slow rates of dynamical variables. In order to do so, one should look for a new coordinates and representation of the governing equations (of the original model) in the form of Singular Perturbed System (SPS) form. Once we found these coordinates, we were able to decompose the original system into slow and fast subsystems which enabled us to apply asymptotic and analytical methods. Let us formalized the general framework theory of the SPVF.

Definition 1 Let $\vec{x} \in R^n$, $\vec{x} = (x_1, x_2, \ldots, x_n)$, $\vec{F} : R^n \to R^n$, $\vec{F} = (F_1, F_2, \ldots, F_n)$ where $\vec{F}_i : R^n \to R, i = 1, 2, \ldots n$.

A general ODE system of order n has the form of: $\dot{\vec{x}} = \vec{F}(\vec{x})$.

Definition 2 Let $\vec{x} \in R^n$, $\vec{x} = \vec{x}_f + \vec{x}_s = (x_{f_1}, x_{f_2}, \ldots, x_{f_{n_f}}, x_{s_1}, x_{s_2}, \ldots, x_{s_{n_s}})$, $\vec{x}_f = (x_{f_1}, x_{f_2}, \ldots, x_{f_{n_f}}, 0, \ldots, 0)$, $\vec{x}_s = (0, \ldots, 0, x_{s_1}, x_{s_2}, \ldots, x_{s_{n_s}})$, where $n_f + n_s = n$.
Let $\vec{F}: R^n \to R^n$, $\vec{F} = \vec{F}_f + \epsilon\vec{F}_s = (F_{f_1}, F_{f_2}, \ldots, F_{f_{n_f}}, \epsilon F_{s_1}, \epsilon F_{s_2}, \ldots, \epsilon F_{s_{n_s}})$, $\vec{F}_f: R^n \to R^{n_f}$, $\vec{F}_s: R^n \to R^{n_s}$ $\vec{F}_f = (F_{f_1}, F_{f_2}, \ldots, F_{f_{n_f}}, 0, \ldots, 0)$, $\vec{F}_f = (0, \ldots, 0, F_{s_1}, F_{s_2}, \ldots, F_{s_{n_s}})$, where $\vec{F}_i: R^n \to R, i \in \{f_1, f_2, \ldots, f_{n_f}, s_1, s_2, \ldots, s_{n_s}\}$.

We call a general ODE system, a Fast-Slow ODE (FS-ODE) if there exists a small parameter ϵ *such that the system has the following form:* $\dot{\vec{x}} = \vec{F}_f(\vec{x})$, $\dot{\vec{x}} = \epsilon\vec{F}_s(\vec{x})$, i.e., $\dot{x}_{f_i} = \vec{F}_{f_i}$ for $1 \le i \le n_f$ and $\dot{x}_{s_i} = \vec{F}_{s_i}$ for $1 \le i \le n_s$. Denote f_{n_f} and s_{n_s} the dimension of the slow and fast ODE subsystem correspondingly.

Definition 3 Given descending in order the set of eigenvalues $\Lambda = \{\lambda_1, \lambda_2, \ldots, \lambda_n\}$. An eigenvalue maximum gap is defined as follows: $\max_i \left\{ \left| \frac{\lambda_{i+1}}{\lambda_i} \right| \right\}$ (we can also define the gap as $\min_i \left\{ \frac{\lambda_i}{\lambda_{i+1}} \right\}$). Let us denote by n_s the index for which we obtain the maximum gap. We call $\Lambda_s = \{\lambda_1, \lambda_2, \ldots, \lambda_{n_s}\}$ slow eigenvalues and the remaining eigenvalues can again be re-indexed to have $\Lambda_f = \{\lambda_1, \lambda_2, \ldots, \lambda_{n_f}\}$ fast eigenvalues, where $n_f + n_s = n$.

Definition 4 Let $A_{n\times m_1}, B_{n\times m_2}$ we denote the Horizontal concatenation of the two matrices by (A ,B), resulting in the matrix of dimension $n \times m$ where $m = m_1 + m_2$.

Method explaining Let $\dot{\vec{x}} = \vec{F}(\vec{x})$ be a general system ODE of order n, that describes a physical phenomena with a hidden hierarchy of rate change of variables. The rate of change is greatly dependent on the choice of the coordinate system. And there are generally two domains of the coordinate system: the domain where the system change is slow and the domain where the change is fast. If in the coordinate system the entire system variables have fast or slow time scales (but not both), then there are no noticeable differences between the rates of change, thus the initial problem is not reduced. Our aim is to find such systems of coordinates in which the ODE system will decompose into slow and fast subsystems i.e., a FS-ODE system. For this purpose, let us choose an arbitrary n vectors $\{\vec{x}_1, \ldots, \vec{x}_n\} \in R^n$. We define the following $n \times n$ matrix T to be the images of these vectors under the vector field $\vec{F}$:

$$T := \begin{pmatrix} F_1(\vec{x}_1) & \ldots & F_1(\vec{x}_n) \\ F_2(\vec{x}_1) & \ldots & F_2(\vec{x}_n) \\ \vdots & \ldots & \vdots \\ F_n(\vec{x}_1) & \ldots & F_n(\vec{x}_n) \end{pmatrix}$$

Let $\Lambda = \{\lambda_1, \ldots, \lambda_n\}$ be the ascending eigenvalues by absolute value of Matrix T, and let $V = \{\vec{v}_1, \ldots, \vec{v}_n\}$ be the eigenvectors respectively. Since the rate of a change of each vector is determined by it eigenvalue, T will be decomposed according to its big and small absolute value of eigenvalues. The maximal gap of eigenvalues can be determined by the $\max_i \left\{ \left| \frac{\lambda_{i+1}}{\lambda_i} \right| \right\}$, we denote this index for which this expression is determined by n_s. By this index we can classify the eigenvalue/eigen vectors into two categories: fast and slow rate. If the index is equal to or smaller than n_s it belong to the slow rate, otherwise it is classified as fast rate.

Let $\Lambda^f = \{\lambda_1^f, \ldots, \lambda_{n_f}^f\}$, $\Lambda^s = \left\{\lambda_1^s, \ldots, \lambda_{n_s}^s\right\}$, $V^f = \{\vec{v}_1^f, \ldots, \vec{v}_{n_f}^f\}$, $V^s = \{\vec{v}_1^s, \ldots, \vec{v}_{n_s}^s\}$

$$\Gamma_f = \begin{pmatrix} \vec{v^f}_{1,1} & \ldots & \vec{v^f}_{n_f,1} \\ \vec{v^f}_{1,2} & \ldots & \vec{v^f}_{n_f,2} \\ \vdots & \ldots & \vdots \\ \vec{v^f}_{1,n} & \ldots & \vec{v^f}_{n_f,n} \end{pmatrix}, \quad \Gamma_s = \begin{pmatrix} \vec{v^s}_{1,1} & \ldots & \vec{v^s}_{n_s,1} \\ \vec{v^s}_{1,2} & \ldots & \vec{v^s}_{n_s,2} \\ \vdots & \ldots & \vdots \\ \vec{v^s}_{1,n} & \ldots & \vec{v^s}_{n_s,n} \end{pmatrix},$$

than we can write:

$$T = \left(\Gamma_{slow}, \Gamma_{fast}\right) \cdot \begin{pmatrix} D_{slow} & 0 \\ 0 & D_{fast} \end{pmatrix} \cdot \left(\Gamma_{slow}, \Gamma_{fast}\right)^{-1},$$

where D_{slow}, D_{fast} are block diagonal matrices with the eigenvalues correspondingly.

The matrix T has eigenvectors that can be divided into two sets: fast eigenvectors and slow eigenvectors, corresponding to big and small absolute value of eigenvalues (the larger the eigen value the greater the rate of change in the direction of matching eigenvector).

According to SPVF decomposition, if the vectors $\{\vec{x}_1, \ldots, \vec{x}_n\}$ are composed of mixed rate of change, the matrix T can be decomposed to the sum $T = T_f + \epsilon T_s$

$$T = \begin{pmatrix} F_{f_1}(\vec{x}_1) & \ldots & F_{f_1}(\vec{x}_n) \\ F_{f_2}(\vec{x}_1) & \ldots & F_{f_2}(\vec{x}_n) \\ \vdots & \ldots & \vdots \\ F_{f_{n_f}}(\vec{x}_1) & \ldots & F_{f_{n_f}}(\vec{x}_n) \end{pmatrix} + \epsilon \begin{pmatrix} F_{s_1}(\vec{x}_1) & \ldots & F_{s_1}(\vec{x}_n) \\ F_{s_2}(\vec{x}_1) & \ldots & F_{s_2}(\vec{x}_n) \\ \vdots & \ldots & \vdots \\ F_{s_{n_s}}(\vec{x}_1) & \ldots & F_{s_{n_s}}(\vec{x}_n) \end{pmatrix},$$

Hence, we can decompose the matrix T to fast and slow subsystems.

The Algorithm for SPVF

The above procedure of SPVF method depends on the choice of linear independent vectors $\{\vec{x}_1, \ldots, \vec{x}_n\}$. The choice of the domain R^n and these points, is a crucial point of the algorithm and should be adapted to every particular model.

The following steps are implemented

1. Select N vectors, uniformly distributed vectors $\Gamma = \{\vec{x}_1, \ldots, \vec{x}_N\}, \vec{x}_i \in R^n$ where $N >> n$.
2. Compute the mean value of the vector filed over the point from step 1: $\bar{F} = \frac{1}{N}\sum_{i=1}^{N} \vec{F}(\vec{x}_i)$,

$$\bar{F} = \begin{pmatrix} \frac{1}{N}\sum_{i=1}^{N} F_1(\vec{x}_i) \\ \frac{1}{N}\sum_{i=1}^{N} F_2(\vec{x}_i) \\ \vdots \\ \frac{1}{N}\sum_{i=1}^{N} F_n(\vec{x}_i) \end{pmatrix} = \frac{1}{N}\sum_{i=1}^{N} \begin{pmatrix} F_1(\vec{x}_i) \\ F_2(\vec{x}_i) \\ \vdots \\ F_n(\vec{x}_i) \end{pmatrix}.$$

3. Define the so-called control set as follows: $\Gamma_{cs} = \{\vec{x}_i \in \Gamma : \|F(x_i)\| > \|\bar{F}\|\}$ for simplicity let reindex $\Gamma_{cs} = \{\vec{x}_1, \ldots, \vec{x}_{N_{cs}}\}$.
4. Build the ordered basis sets:

   $B_i = \{\vec{x}_{(i-1)\cdot n+1}, \ldots, \vec{x}_{i\cdot n}\}$ with the corresponding matrix

$$A_i = \begin{pmatrix} x_{1,(i-1)\cdot n+1} & \ldots & x_{1,i\cdot n} \\ x_{2,(i-1)\cdot n+1} & \ldots & x_{2,i\cdot n} \\ \vdots & \ldots & \vdots \\ x_{n,(i-1)\cdot n+1} & \ldots & x_{n,i\cdot n} \end{pmatrix}$$

   and let $\mathbb{B} = \{B_1, B_2, \ldots, B_m\}$, $\mathbb{A} = \{A_1, A_2, \ldots, A_m\}$ where $m = \lfloor \frac{N_{cs}}{n} \rfloor$.
5. Select only the reference basis set from step 4 which have $|Det(A_i)|$ above the average level over all determinate basis i.e., let $\Omega = \frac{1}{m}\sum_{i=1}^{m} |Det(A_i)|$, then the reference basis is $B_{rb} = \{B_i : |Det(A_i)| \geq \Omega, i = 1, \ldots, m\}$. Again let us reindex, $B_{rb} = \{B_1, B_2, \ldots, B_k\}$ with the matching reindex of vectors $\vec{x}$.

6. For each $i = 1, 2, \ldots, k$ compute the eigenvalues of following matrix T_i that correspond to the matching basis B_i,

$$T_i = \begin{pmatrix} F_1(\vec{x}_{(i-1)\cdot n+1}) & \ldots & F_1(\vec{x}_{i\cdot n}) \\ F_2(\vec{x}_{(i-1)\cdot n+1}) & \ldots & F_2(\vec{x}_{i\cdot n}) \\ \vdots & \ldots & \vdots \\ F_n(\vec{x}_{(i-1)\cdot n+1}) & \ldots & F_n(\vec{x}_{i\cdot n}) \end{pmatrix}.$$

7. Let $\{\lambda_1^i, \lambda_2^i, \ldots, \lambda_n^i\}$ be in ascending ordered eigenvalues of T_i. For each T_i we compute max gap as:

$$gap_{max_i} = \max_n \left(\left| \lambda_{n+1}^i(T_i) \right| / \left| \lambda_n^i(T_i \right| \right).$$

8. Denote by i_{max} the index for which gap_{max_i} is maximal. The eigenvectors of $T_{i_{max}}$, $\{\vec{v}_1^{i_{max}}, \vec{v}_2^{i_{max}}, \ldots, \vec{v}_n^{i_{max}}\}$, that correspond to $\{\lambda_1^{i_{max}}, \lambda_2^{i_{max}}, \ldots, \lambda_n^{i_{max}}\}$ consist of the desired coordinate system. Let n_s-be the index for which $\left(\left| \lambda_{n+1}^{i_{max}}(T_{i_{max}}) \right| / \left| \lambda_n^{i_{max}}(T_{i_{max}} \right| \right)$ is maximal. Then the vectors
$\{\vec{v}_1^{i_{max}}, \vec{v}_2^{i_{max}}, \ldots, \vec{v}_{n_s}^{i_{max}}\}$ and, $\{\vec{v}_{n_s+1}^{i_{max}}, \vec{v}_{n_s+2}^{i_{max}}, \ldots, \vec{v}_n^{i_{max}}\}$ are the new slow and fast vectors of the slow and fast system correspondingly.
9. Rewrite the original system in the new coordinate $\{\vec{v}_1^{i_{max}}, \vec{v}_2^{i_{max}}, \ldots, \vec{v}_n^{i_{max}}\}$.

Comment: In general, when one applies the SPVF algorithm, especially in complex systems, the eigenvalues of the matrix T can be complex numbers. In order to overcome this problem one should take in the algorithm the square root of the eigenvalues of the matrix TT^* to be the practical eigenvalues of the considered problem (since TT^* is symmetric it has real eigenvalues).

Application of the SPVF Method

In this section we applied the SPVF method to the thermal explosion of monodisperse fuel spray.

The Monodisperse Fuel Spray Model

In this section we apply the SPVF to the model of thermal explosion of monodisperse fuel spray. The physical assumptions of the physical model are as follows: The droplet boundaries are assumed to be on the saturation line i.e., the liquid temperature is constant and equal to the liquid saturation temperature. The combustible liquid droplets are considered to comprise a polydisperse spray. The assumption of the quasi-steady-state approximation is valid for the vaporizing droplets. The thermal conductivity of the liquid phase is much greater than that of the gas phase. Thus, the heat transfer coefficient in the liquid gas mixture is supposed to be defined by the thermal properties of the gas phase. An adiabatic approach is applied. Because the ignition time is a very short period, the adiabatic assumption is valid. During this period, there is almost no heat transfer out of the system. For thermal explosion processes, the pressure change in the reaction volume and its influence on the combustion process is neglected. The combustion reaction is modeled as a first order, highly exothermic chemical reaction. The model has the form of a system of non-linear ordinary differential equations. Moreover, it contains an energy equation for the reacting gas, mass equations for the liquid droplets of m different sizes and a concentration equation for the reacting gas mixture.

Under these assumptions, the system of the governing equations as given in [27] is:

$$\frac{dT_g}{dt} = \frac{\alpha_g \mu_f Q_f A C_f e^{\left(-\frac{E}{BT_g}\right)}}{\alpha_g \rho_g c_{pg}} - \frac{4\pi\lambda_g (T_g - T_d) R_{d_i} n_{d_i}}{\alpha_g \rho_g c_{pg}} \equiv F_1\left(T_g, R_{d_i}, C_f\right), \quad (1)$$

$$\frac{d(R_{d_i}^2)}{dt} = -\frac{2\lambda_g}{\rho_L L}(T_g - T_d) \equiv F_2\left(T_g, R_{d_i}, C_f\right),\ i = 1, \ldots, m,\ (m\ equations) \quad (2)$$

$$\frac{dC_f}{dt} = -AC_f e^{\left(-\frac{E}{BT_g}\right)} + \frac{4\pi\lambda_g (T_g - T_d) R_{d_i} n_{d_i}}{L\alpha_g \mu_f} \equiv F_3\left(T_g, R_{d_i}, C_f\right). \quad (3)$$

In our notations $\vec{F} = (F_1, F_2, F_3)$.
The initial conditions are:

$$at\ t = 0:\ T_g(t = 0) = T_{g0} = T_{d_i},\ R_{d_i} = R_{d_{i0}},\ C_f = C_{f0}. \quad (4)$$

Equations (1)–(3) include an energy equation for the reacting gas, a mass equation for liquid droplets, and a concentration equation for the reacting gas mixture, respectively.

Preliminary Results

Monodisperse Model Experimental Data

The initial conditions are: $T_{g0} = 860$, $R_{di0} = 10^{-4}$ and $C_{f0} = 120$.
The domain of the results for the temperature is $[0, 5.6] \times [860, 1120]$, for the radius is $[0, 5.6] \times [0, 10^{-4}]$ and for the concentration is $[0, 5.6] \times [0, 135]$. The results shown in Figs. 1, 2 and 3. Figure 1 present the solution profile of the temperature of monodisperse model for three different fuel types ($Decane$, $Heptane$ and $Tetralin$). According to this figure the thermal explosion of the monodisperse spray occurs after $\approx [4.2s - 5.3s]$, i.e., the thermal explosion for $Decane$ occurs after $4.2s$, for $Heptane$ after $4.8s$ and for $Tetralin$ after $5.3s$. The evaporation of the radius R_d (see Fig. 2) corresponds to the explosion time for the solution profile of the temperature, i.e., for example the radius of the $Decane$ fuel, that start at the initial radius $R_{d0} = 10^{-4}$, decreases to zero after $\approx 4.3s$ and so on. The solution profile of the concentration C_f (see Fig. 3) is also coherent to the solution profile of the temperature and radius. For example concentration of the $Decane$ that start at $120 kmol m^{-3}$ decrease to zero at the explosion time after $\approx$4.12 s.

Application of the SPVF Algorithm

The data for the SPVF algorithm: $N = 20,000$ and $n = 3$. The results of the SPVF algorithm i.e., the eigenvalues and the corresponds eigenvectors are summarized below:

$$\lambda_1 = 0.00004 \longleftrightarrow \vec{v}_1 = (-0.00001, 1, -0, 00003)^T$$
$$\lambda_2 = 0.00004 \longleftrightarrow \vec{v}_2 = (-0.7194, -0.00007, -0.6946)^T$$
$$\lambda_3 = 0.00004 \longleftrightarrow \vec{v}_3 = (-0.6946, 0.00007, 0.7194)^T$$

According to the SPVF theory, the eigenvector $\vec{v}_3$, that corresponds to the largest eigenvalue λ_3 indicates the fast direction of the system in the new coordinates. λ_1 and λ_2 correspond to the slow direction of the system since they are at approximately the same order and $\lambda_1, \lambda_2 << \lambda_3$.

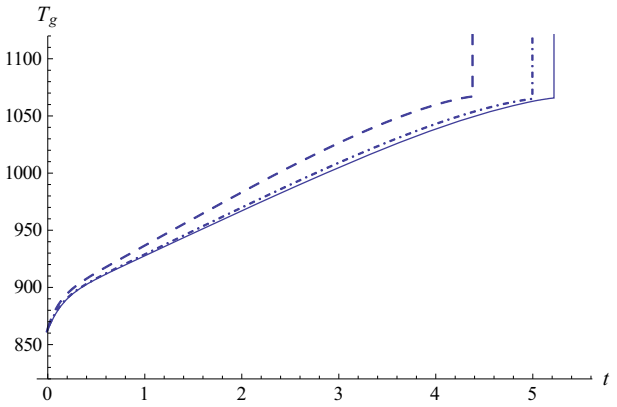

Fig. 1 The solution profile of the temperature of monodisperse model for three different fuel types applying numerical simulation. *Dash line* decane, *dash-dot line* heptane and *solid line* tetralin

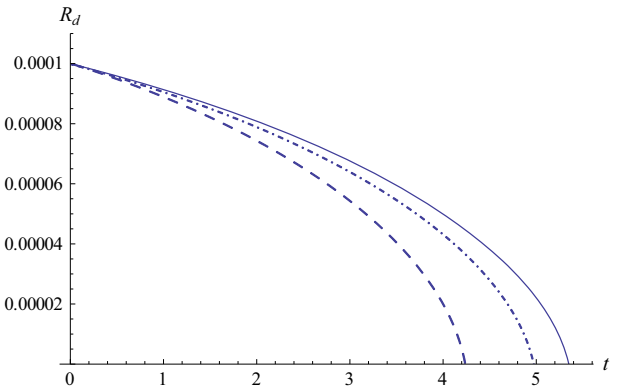

Fig. 2 The solution profile of the radius of monodisperse model for three different fuel types applying numerical simulation. *Dash line* decane, *dash-dot line* heptane and *solid line* tetralin

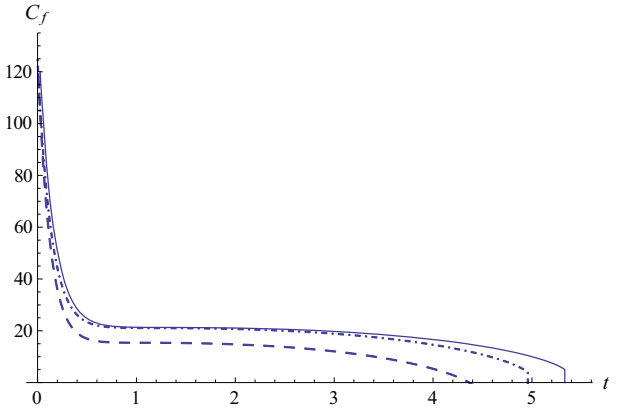

Fig. 3 The solution profile of the cencentration of monodisperse model for three different fuel types applying numerical simulation. *Dash line* decane, *dash-dot line* heptane and *solid line* tetralin

The next step is to rewrite the monodisperse model in a new coordinate using the above eigenvectors. Hence, let us write:

$$\begin{pmatrix} x \\ y \\ z \end{pmatrix} = \begin{pmatrix} -0.00001 & 1 & -0.00003 \\ -0.7194 & -0.00007 & -0.6946 \\ -0.6946 & 0.00007 & 0.7194 \end{pmatrix} \cdot \begin{pmatrix} T_g \\ R_d \\ C_f \end{pmatrix} \tag{5}$$

After the above multiplication the aim of the next step is to write the temperature, radius, and the concentration as a function of the new coordinates, i.e., $T_g = T_g(x, y, z)$, $R_d = R_d(x, y, z)$, $C_f = C_f(x, y, z)$.
From Eq. (6) we obtain the following system:

$$\begin{aligned} \frac{dx}{dt} &= -0.00001 \cdot \frac{dT_g}{dt} + \frac{dR_d}{dt} - 0.00003 \cdot \frac{dC_f}{dt}, \\ \frac{dy}{dt} &= -0.7194 \cdot \frac{dT_g}{dt} - 0.00007 \cdot \frac{dR_d}{dt} - 0.6946 \cdot \frac{dC_f}{dt}, \\ \frac{dz}{dt} &= -0.6946 \cdot \frac{dT_g}{dt} + 0.00007 \cdot \frac{dR_d}{dt} + 0.7194 \cdot \frac{dC_f}{dt}, \end{aligned} \tag{6}$$

now substitute the expressions of $\frac{dT_g}{dt}$, $\frac{dR_d}{dt}$ and $\frac{dC_f}{dt}$ from the monodisperse model (1)–(3) into the Eq. (6), i.e., substitute $F_1\left(T_g, R_{d_i}, C_f\right)$, $F_2\left(T_g, R_{d_i}, C_f\right)$ and $F_3\left(T_g, R_{d_i}, C_f\right)$ from Eqs. (1)–(3) instead of the expressions $\frac{dT_g}{dt}$, $\frac{dR_d}{dt}$ and $\frac{dC_f}{dt}$ correspondingly into Eq. (6). Now substitute $T_g = T_g(x, y, z)$, $R_d = R_d(x, y, z)$, $C_f = C_f(x, y, z)$ into F_1, F_2 and F_3 and obtain the monodisperse fuel spray model in the new coordinate (x, y, z) in the following form:

$$\begin{aligned} \frac{dx}{dt} &= -0.00001 \cdot F_1\left(T_g(x, y, z), R_{d_i}(x, y, z), C_f(x, y, z)\right) \\ &\quad + F_2\left(T_g(x, y, z), R_{d_i}(x, y, z), C_f(x, y, z)\right) \\ &\quad - 0.00003 \cdot F_3\left(T_g(x, y, z), R_{d_i}(x, y, z), C_f(x, y, z)\right) \equiv \tilde{F}_1(x, y, z), \\ \frac{dy}{dt} &= -0.7194 \cdot F_1\left(T_g(x, y, z), R_{d_i}(x, y, z), C_f(x, y, z)\right) \\ &\quad - 0.00007 \cdot F_2\left(T_g(x, y, z), R_{d_i}(x, y, z), C_f(x, y, z)\right) \\ &\quad - 0.6946 \cdot F_3\left(T_g(x, y, z), R_{d_i}(x, y, z), C_f(x, y, z)\right) \equiv \tilde{F}_2(x, y, z), \\ \frac{dz}{dt} &= -0.6946 \cdot F_1\left(T_g(x, y, z), R_{d_i}(x, y, z), C_f(x, y, z)\right) \\ &\quad + 0.00007 \cdot F_2\left(T_g(x, y, z), R_{d_i}(x, y, z), C_f(x, y, z)\right) \\ &\quad + 0.7194 \cdot F_3\left(T_g(x, y, z), R_{d_i}(x, y, z), C_f(x, y, z)\right) \equiv \tilde{F}_3(x, y, z). \end{aligned} \tag{7}$$

The Physical Domain of the Model in the New Coordinates

In order to solve the model in the new coordinates we should transform the physical domain of the original model under the considered transformation (see Figs. 4, 5, 6).
For each coordinate, we select the two vectors according to the value of the transformed matrix, such that the multiplication will result in the minimum and maximum values. i.e.,

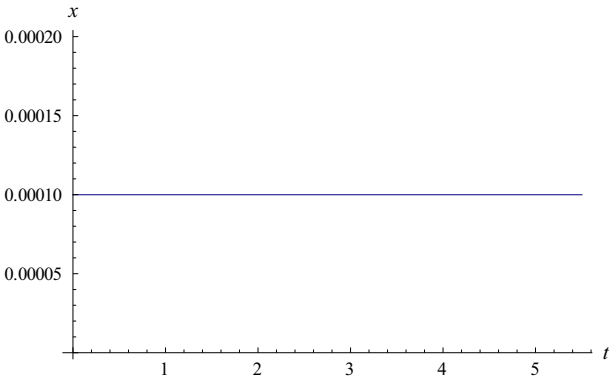

Fig. 4 The solution profile of the x-coordinate: the asymptotic case when $x \approx R_d$ according to Eq. (5)

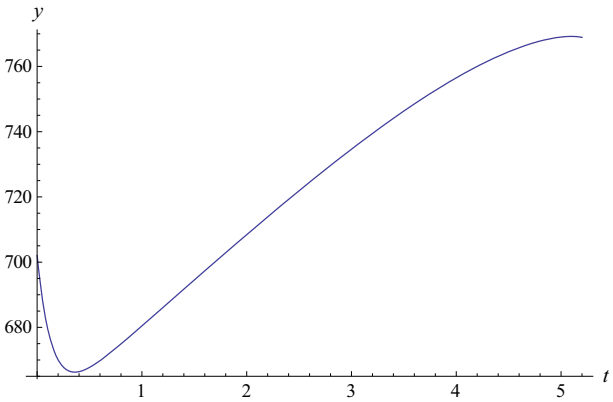

Fig. 5 The solution profile of the y-coordinate: the asymptotic case when for convenience we take the eigenvector $\vec{v}_2$ as $-\vec{v}_2$ (i.e., we take the eigenvalue λ_2 as $-\lambda_2$) and from Eq. (5) we obtained $y \approx 0.7194 \cdot T_g + 0.6946 \cdot C_f$

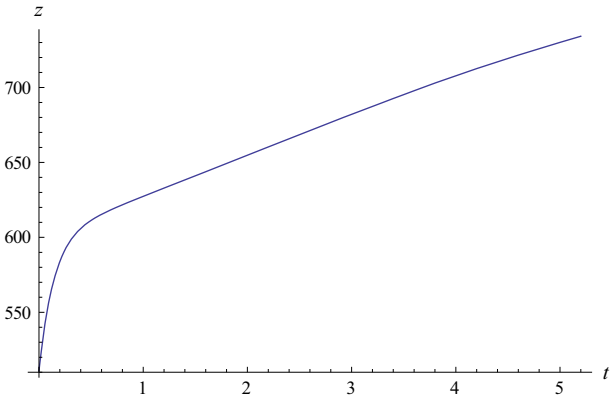

Fig. 6 The solution profile of the z-coordinate: the asymptotic case when for convenience we take the $\vec{v}_3$ as $-\vec{v}_3$ (i.e., we take the eigenvalue λ_3 as $-\lambda_3$) and from Eq. (5) we obtained $z \approx 0.6946 \cdot T_g - 0.7194 \cdot C_f$

x-coordinate:

$$\begin{pmatrix} -0.00001 & 1 & -0.00003 \\ -0.7194 & -0.00007 & -0.6946 \\ -0.6946 & 0.00007 & 0.7194 \end{pmatrix} \cdot \begin{pmatrix} 0 \\ 10^{-4} \\ 0 \end{pmatrix} = \begin{pmatrix} 0.0001 \\ -7 \cdot 10^{-9} \\ 7 \cdot 10^{-9} \end{pmatrix} \tag{8}$$

$$\begin{pmatrix} -0.00001 & 1 & -0.00003 \\ -0.7194 & -0.00007 & -0.6946 \\ -0.6946 & 0.00007 & 0.7194 \end{pmatrix} \cdot \begin{pmatrix} 5000 \\ 0 \\ 200 \end{pmatrix} = \begin{pmatrix} -0.056 \\ -3735.92 \\ -3329.12 \end{pmatrix} \tag{9}$$

this means that the physical domain of the new x-coordinate is $x \in [-0.056, 0.0001]$.
y-coordinate:

$$\begin{pmatrix} -0.00001 & 1 & -0.00003 \\ -0.7194 & -0.00007 & -0.6946 \\ -0.6946 & 0.00007 & 0.7194 \end{pmatrix} \cdot \begin{pmatrix} 0 \\ 0 \\ 0 \end{pmatrix} = \begin{pmatrix} 0 \\ 0 \\ 0 \end{pmatrix} \tag{10}$$

$$\begin{pmatrix} -0.00001 & 1 & -0.00003 \\ -0.7194 & -0.00007 & -0.6946 \\ -0.6946 & 0.00007 & 0.7194 \end{pmatrix} \cdot \begin{pmatrix} 5000 \\ 10^{-4} \\ 200 \end{pmatrix} = \begin{pmatrix} -0.0559 \\ -3735.92 \\ -3329.12 \end{pmatrix} \tag{11}$$

this means that the physical domain of the new y-coordinate is $y \in [-3735.92, 0.0001]$.
z-coordinate:

$$\begin{pmatrix} -0.00001 & 1 & -0.00003 \\ -0.7194 & -0.00007 & -0.6946 \\ -0.6946 & 0.00007 & 0.7194 \end{pmatrix} \cdot \begin{pmatrix} 0 \\ 10^{-4} \\ 200 \end{pmatrix} = \begin{pmatrix} -0.0059 \\ -138.92 \\ 143.88 \end{pmatrix} \tag{12}$$

$$\begin{pmatrix} -0.00001 & 1 & -0.00003 \\ -0.7194 & -0.00007 & -0.6946 \\ -0.6946 & 0.00007 & 0.7194 \end{pmatrix} \cdot \begin{pmatrix} 5000 \\ 0 \\ 0 \end{pmatrix} = \begin{pmatrix} -0.05 \\ -3597 \\ -3473 \end{pmatrix} \tag{13}$$

this means that the physical domain of the new z-coordinate is $z \in [-3473, 143.88]$.

Stability

According to the method of integral invariant method the analysis of the system dynamics is reduced to the analysis on the slow manifold. The slow manifold is determined, by taking the derivative of the fast variable to zero in Eq. (7) i.e., $dz/dt = 0 \Rightarrow \tilde{F}_3(x, y, z) = 0$.

In order to find the stable/ unstable points of the slow manifold, one should compute the derivative of the slow manifold with respect to the fast variable, i.e., $\partial_z \tilde{F}_3(x, y, z)$. We substitute each point from the slow manifold into the expression $\partial_z \tilde{F}_3$. Points are stable when $\partial_z \tilde{F}_3 < 0$. In Fig. 7 we presented the slow manifold of the system (7). Figure 8 presents the stability points of the system (7), Fig. 9 presents the non-stability points of the system (7), and Fig. 10 presents both the stability and non-stability points of the system (7).

Steady State Approximation

Given a system of ordinary differential equations, the behavior of a dynamic system is related to the systems' variables. As in our case the system is approximated by linear ordinary differential equations as presented in Eq. (7). When this is the case, classical or closed form solutions can be obtained. For the general case of non-linear differential equations, solutions must be sought through the use of simulations by analog computation methods or by numerical integration techniques carried out using computers. Although any problem can

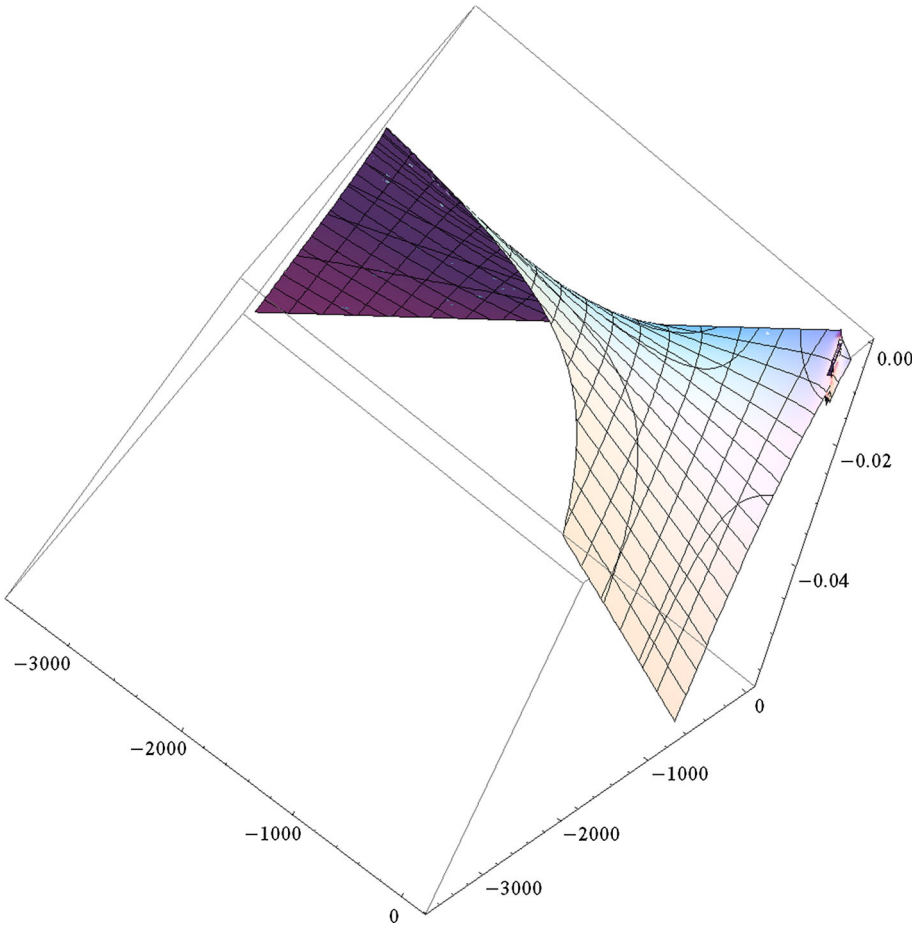

Fig. 7 The slow manifold of the system (7) the manifold $\tilde{F}_3\,(x, y, z)$

be solved by these simulations methods, the insight that can be derived from linear system analysis is invaluable as a guide to control system design and performance evaluations. One method that can give an insight into the dynamical of the linear system (7) is the steady state analysis.

In general, given a system of first order ordinary differential equations $\vec{x}' = \vec{f}(\vec{x})$ the $\vec{x}$-*nullcline* is the set of points which satisfy $\vec{f} = 0$. The intersection point of all the nullclines is called the $equilibrium\ point$ or $fixed\ point$ of the considered system. The Jacobian matrix with constant entries, is identified with the matrix of a linear systems. Near a fixed point which is denoted by (x^*, y^*, z^*), the dynamics of the nonlinear system are qualitatively similar to the dynamics of the linear system associated with the Jacobian matrix $J = J(x^*, y^*, z^*)$, provided its eigenvalues λ_j's have nonzero real parts. Fixed points with a Jacobian matrix such that $Re(\lambda_j) \neq 0$ are called hyperbolic fixed points. Otherwise, they are non-hyperbolic fixed points, whose stabilities must be determined directly.

The physical meaning of stability is the ability of a system to return to its steady state when subjected to a disturbance, i.e., the non-linear system's phase portrait near the fixed

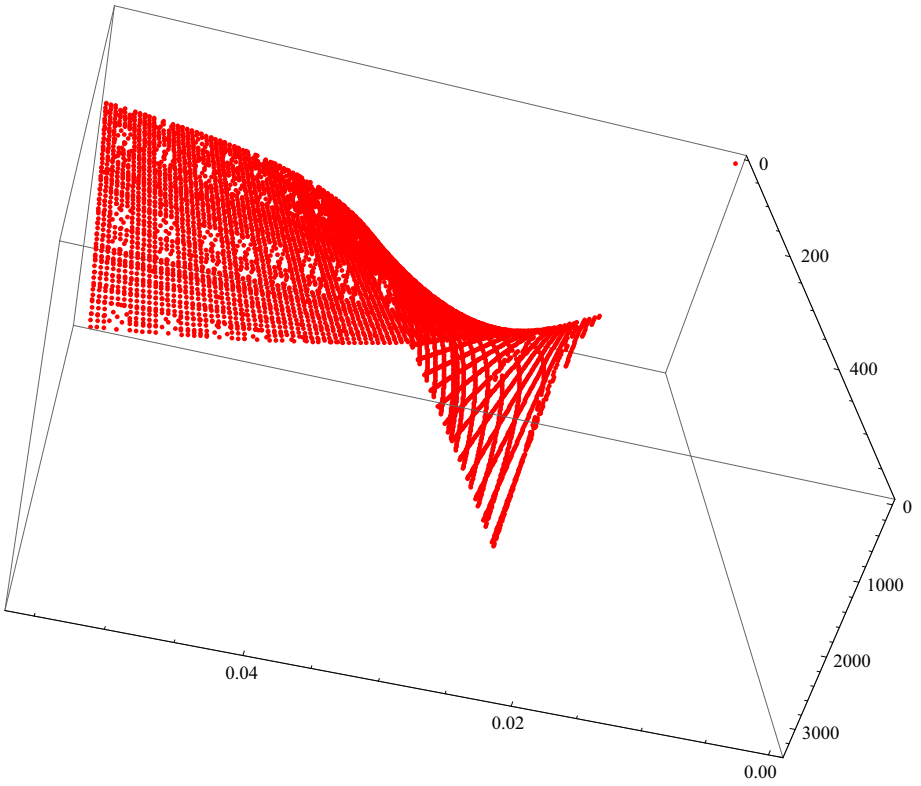

Fig. 8 The stability points of the slow manifold of the system (7) with $\partial_z \tilde{F}_3\,(x, y, z) < 0$

point is topologically unchanged due to small perturbations, and its dynamics are structurally stable or robust. Hence, the equilibria of the system (7) are found by setting all derivatives to zero and solving for (x^*, y^*, z^*), with star notation indicating that the variables are at their equilibrium values. When analyzing the stability of each equilibrium of the above system, one can examine the Jacobian of the system (7) given by:

$$J = J(x^*, y^*, z^*) = \frac{\partial(\tilde{F}_1, \tilde{F}_2, \tilde{F}_3)}{\partial(x, y, z)}. \tag{14}$$

In order to determine if the stability of the points that are obtained from the solution of the system

$$\begin{cases} \tilde{F}_1 = 0 \\ \tilde{F}_2 = 0 \\ \tilde{F}_3 = 0 \end{cases} \tag{15}$$

are stable, we substituted these points in J and computed the eigenvalues of J for each point. The points from this steady state system are in 3 dimensional space. So a point is stable if all of its 3 eigenvalues are negative. In Fig. 11 we presented the steady state surface as the intersections of the surfaces $(\tilde{F}_1, \tilde{F}_2, \tilde{F}_3)$. Figure 12 presented the stable points of this surface.

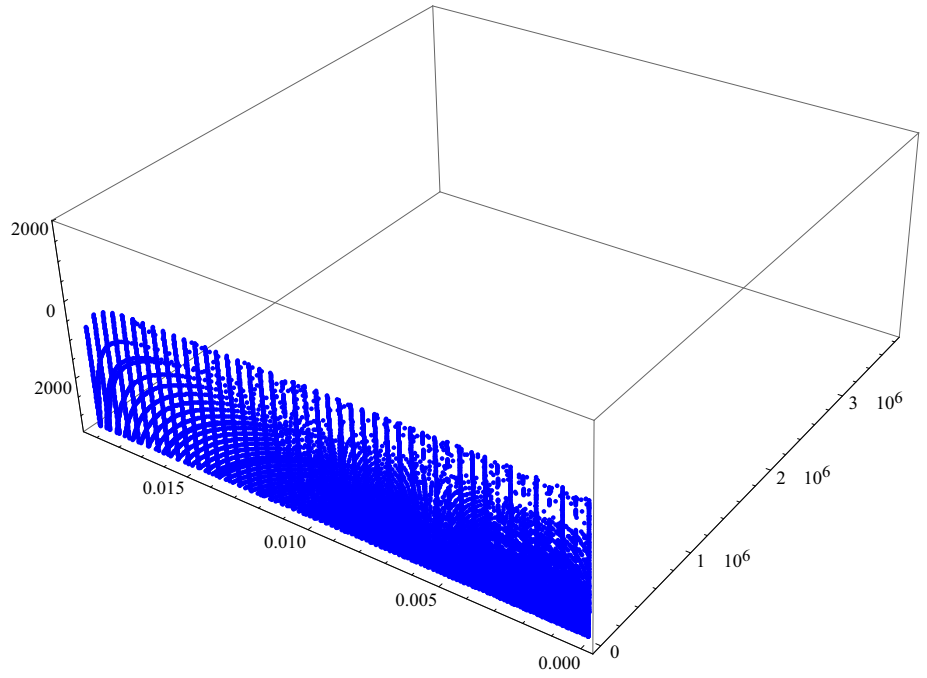

Fig. 9 The non-stability points of the slow manifold of the system (7) with $\partial_z \tilde{F}_3\,(x, y, z) > 0$

The initial conditions are obtained from Eq. (8) when substituting $t = 0$. The above model (7) is a system of ordinary linear differential equations that can be solved using simple code in Matlab. The results are presented in Figs. 4, 5 and 6. Figure 4 presented the solution profile of the system (7) for the x-coordinate. In the asymptotic case the new coordinate x is constant which is compatible with the solution profile of the radius of the monodisperse model (see Fig. 2), i.e., $\frac{\Delta R_d}{\Delta t} \approx \frac{0.0001-0}{5.2-0} = 0.0000192 \Longrightarrow \frac{dR_d}{dt} \approx 0$. Figure 5 presented the solution profile of the system (7) for the y-coordinate. In the asymptotic case, from the system (8), we have $y \approx 0.7194 \cdot T_g + 0.6946 \cdot C_f$, i.e., the new coordinate y is a combination (sum) of the temperature and the concentration of the monodisperse spray model. The coefficients of this combination (which are the first and the last coordinates of the eigenvector $\vec{v}_2$) have the proportion $\frac{0.7194}{0.6946} \approx 1$. This means that if we sum the solution profile of the temperature and the solution profile of the concentration point by point we obtain the graph of y, and indeed Fig. 5 is coherent with this analysis. For example, at the time $2.45s \Longrightarrow T_g = 982$ and $C_f = 214.01$ then $0.7194 \cdot T_g + 0.6946 \cdot C_f = 716.182$, and the y-coordinate at $2.45s$ is 717.223 as expected (see Fig. 5). The new coordinate z is a combination (difference) between the temperature and the concentration. The same analysis can be done for the z-coordinate, (see Fig. 6).

New general results Given the model of monodisperse fuel spray (1)–(3) the standard machinery to analyze the model is to transfer the model into a non-dimensional one in the form of Singular Perturbed System (SPS), i.e., a system with explicit small parameter which decomposed the system into fast and slow subsystems.

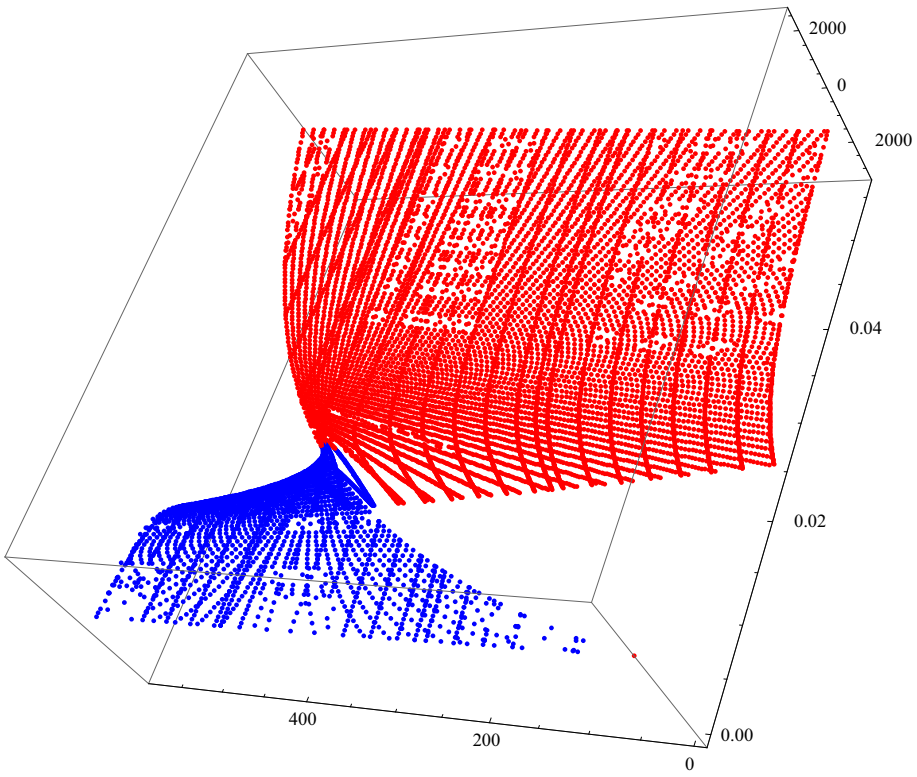

Fig. 10 The stability and non-stability points of the system (7)

Considered the system (1)–(3) in non-dimensional SPS form as:

$$\begin{aligned}
\frac{d\theta_g}{d\tau} &= \tilde{F}_1\left(\frac{1}{\epsilon}, \theta_g, r_{d_i}, \eta_f\right), \\
\frac{dr_{d_i}}{d\tau} &= \tilde{F}_2\left(\theta_g, r_{d_i}, \eta_f\right), \\
\frac{d\eta_f}{d\tau} &= \tilde{F}_3\left(\theta_g, r_{d_i}, \eta_f\right),
\end{aligned} \tag{16}$$

where τ is the dimensionless time, θ_s is the gas temperature, r_{d_i} is the droplets radii, η_f is the fuel concentration, and ϵ is the small parameter of the system. Once the system is presented as SPS system one can applied various asymptotic method such as the method of integral manifolds, different perturbation methods, etc.

According to the system (16) one can see that the fast variable of the system is the gas temperature θ_g. Since the system is adiabatic, hence the energy integral, which represents the energy conservation law, is exists. Hence, by applying the energy integral procedure one can obtain an explicit expression for the concentration as the function of the gas temperature and the radius, $\eta_f = \eta_f(\theta_g, r_{d_i})$. This enable one to reduced the considered system from three equations into two equations only in the form of

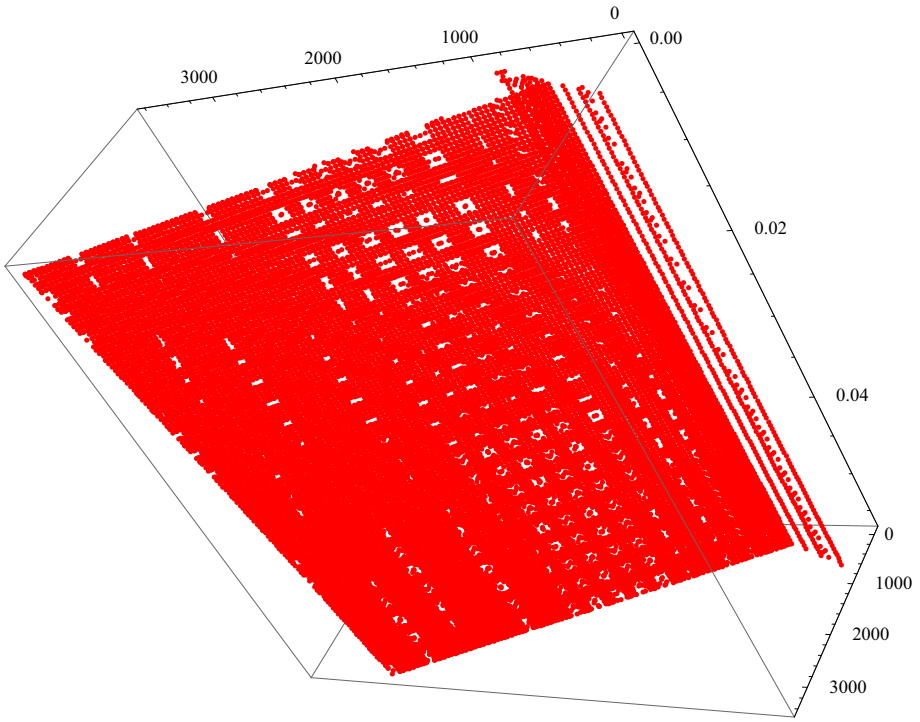

Fig. 11 The steady state surface of the system (7), i.e., the intersections of the surfaces $\tilde{F}_1(x, y, z) = \tilde{F}_2(x, y, z) = \tilde{F}_3(x, y, z) = 0$

$$\begin{aligned} \frac{d\theta_g}{d\tau} &= \tilde{F}_1\left(\frac{1}{\epsilon}, \theta_g, r_{d_i}, \eta_f\left(\theta_g, r_{d_i}\right)\right), \\ \frac{dr_{d_i}}{d\tau} &= \tilde{F}_2\left(\theta_g, r_{d_i}, \eta_f\left(\theta_g, r_{d_i}\right)\right), \\ \eta_f &= \eta_f\left(\theta_g, r_{d_i}\right). \end{aligned} \tag{17}$$

According to the form of the above system, the fast variable of the system is only the gas temperature (the droplets radii is the slow one). Hence, the main problem when applying the above procedure is the loss of the physical properties of the variables of the system. And indeed, when we apply the SPVF algorithm the dimensional monodisperse model Equations, (1)–(3), we receive that the fast direction of the system is the combination between the gas temperature T_g and the concentration C_f in the form of $-0.6946 \cdot T_g + 0.7194 \cdot C_f$ (which means increasing temperature and decreasing the concentration) or one can choose the option of $0.6946 \cdot T_g - 0.7194 \cdot C_f$. This means that the fast variables of the original system is in the direction of the gas temperature T_g and in the direction of the fuel concentration C_f. This information of the fast physical variable, the concentration, is loss when applying the energy integral.

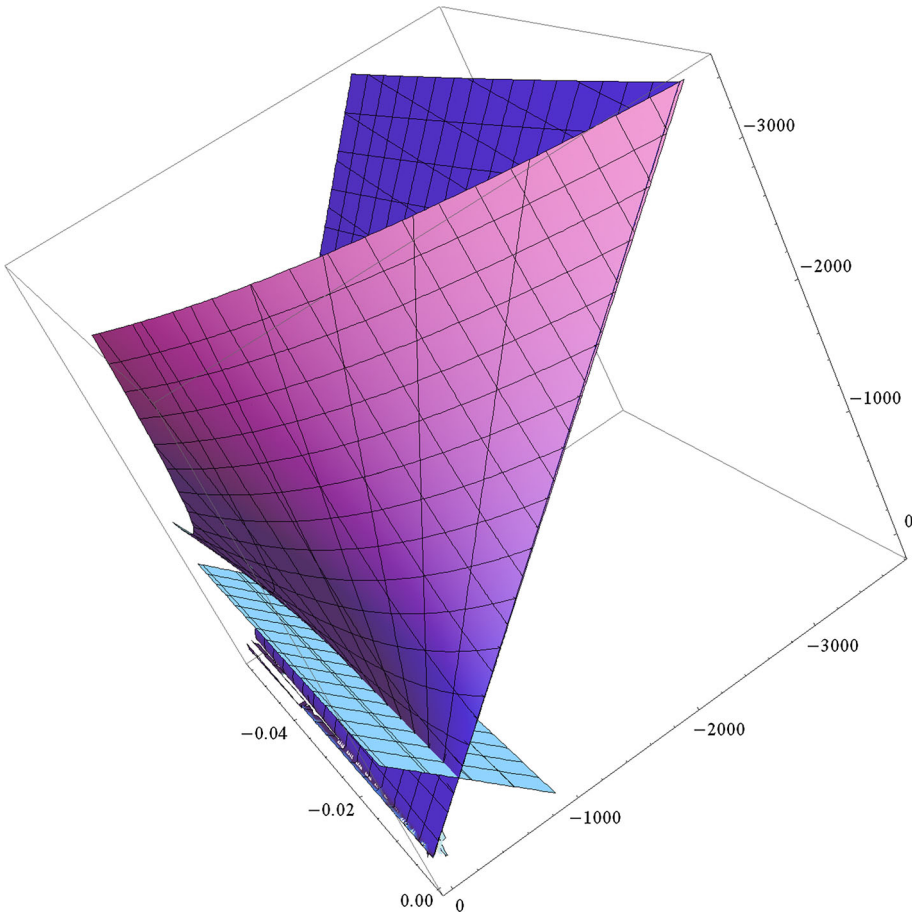

Fig. 12 The stability of the steady state surface where all the eigenvalues of the Jacobian matrix are negative

Conclusions

In our research we presented the theoretical framework and the algorithm of singular perturbed vector field (SPVF) and its application to the problem of thermal explosion of a monodisperse spray model. Given the monodisperse model, the hierarchical properties are hidden. By applying the SPVF method, we have rewritten the monodisperse model in a new coordinate which reveals the combustion process of the model. This enables us to decompose the system dynamics of the monodisperse model into the so-called "slow" and "fast" motions.

The new coordinates are a combination of the original variables of the system. This can be useful for engineering applications. For example, the y-coordinate is a combination of 70% of the gas temperature and 69% of the concentration. This combination can be mixing for an optimal combustion of the monodisperse spray.

In addition the main result of the SPVF method is that it enables the reduction the dimension of the system, and hence to reduce the numerical and analytical computations which are time-consuming on the computer.

References

1. Gol'dshtein, V.M., Sobolev, V.A.: Singularity theory and some problems of functional analysis. Am. Math. Soc. **153**(2), 73–92 (1992)
2. Babushok, V.I., Gol'dshtein, V.M.: Structure of the thermal explosion limit. Combust. Flame **72**(3), 221–226 (1988)
3. McIntosh, A.C., Gol'dshtein, V.M., Goldfarb, I., Zinoviev, A.: Thermal explosion in a combustible gas containing fuel droplets. Combust. Theory Model. **2**(2), 153–165 (1998)
4. Goldfarb, I., Gol'dshtein, V.M., Kuzmenko, G., Greenberg, B.J.: Monodisperse spray effects on thermal explosion in a gas. In: HTD-352 Proc. ASME Heat Transfer Division, ASME Int. Congress and Exposition, Dallas, TX, vol. 2, pp. 199–206 (1997)
5. Roussel, M.R., Fraser, S.J.: Geometry of the steady-state approximation: perturbation and accelerated convergence methods. J. Chem. Phys. **93**, 47–63 (1990)
6. Roussel, M.R., Fraser, S.J.: Accurate steady-state approximations: implications for kinetics experiments and mechanism. J. Chem. Phys. **95**, 8762–8770 (1991)
7. Roussel, M.R., Fraser, S.J.: Global analysis of enzyme inhibition kinetics. J. Chem. Phys. **97**, 8316–8327 (1993)
8. Roussel, M.R., Fraser, S.J.: Invariant manifold methods for metabolic model reduction. Chaos **11**, 196–206 (2001)
9. Zagaris, A., Kaper, H.G., Kaper, T.J.: Analysis of the computational singular perturbation reduction method for chemical kinetics. J. Nonlinear Sci. **14**, 59–91 (2004)
10. Zagaris, A., Kaper, H.G., Kaper, T.J.: Fast and slow dynamics for the computational singular perturbation method. Soc. Ind. Appl. Math. **2**(4), 613–638 (2004)
11. Berglunda, N., Gentzd, B.: Geometric singular perturbation theory for stochastic differential equations. J. Diff. Equ. **191**(1), 1–54 (2003)
12. Fenichel, N.: Geometric singular perturbation theory for ordinary differential equations. J. Diff. Equ. **31**(1), 53–98 (1979)
13. Jones, C.K.: Geometric singular perturbation theory. Dynamical Systems, 1609 of the series Lecture Notes in Mathematics, pp 44–118 (2006)
14. Maas, U., Pope, S.B.: Implementation of simplified chemical kinetics based on intrinsic low-dimensional manifolds (PDF). In: Symposium (International) on Combustion. Twenty-Fourth Symposium on Combustion vol. 24(1), pp. 103–112 (1992)
15. Maas, U., Pope, S.B.: Simplifying chemical kinetics: intrinsic low-dimensional manifolds in composition space. Combust. Flame **88**(3–4), 239–264 (1992)
16. Bongers, H., Van Oijen, J.A., De Goey, L.P.H.: Intrinsic low-dimensional manifold method extended with diffusion. Proc. Combust. Inst. **29**(1), 1371–1378 (2002)
17. Alison, S.T., Whitehouse, L., Richard, L.: The estimation of intrinsic low dimensional manifold dimension in atmospheric chemical reaction systems. In: Bruno, S. (ed.) Air Pollution Modelling and Simulation, pp. 245–263. Springer, Berlin Heidelberg (2002)
18. Hans, G.K., Tasso, J.K.: Asymptotic analysis of two reduction methods for systems of chemical reactions. Physica D **165**, 66–93 (2002)
19. Bykov, V., Maas, U.: Reaction-diffusion manifolds and global quasi-linearization: two complementary methods for mechanism reduction. Open Thermodyn J **7**, 92–100 (2013)
20. Bykov, V., Griffiths, J.F., Piazzesi, R., Sazhin, S.S., Sazhina, E.M.: The application of the global quasi-linearisation technique to the analysis of the cyclohexane/air mixture autoignition. Appl. Math. Comput. **219**(14), 7338–7347 (2013)
21. Bykov, V., Gol'dshtein, V., Maas, U.: Simple global reduction technique based on decomposition approach. Combust. Theory Model. **12**(2), 389–405 (2008)
22. Bykov, V., Gol'dshtein, V.: On a decomposition of motions and model reduction. J. Phys. Conf. Ser. **138**, 1–15 (2008)
23. Bykov, V., Goldfarb, I., Gol'dshtein, V.: Singularly perturbed vector fields. J. Phys. Conf. Ser. **55**, 28–44 (2006)
24. Bykov, V., Maas, U.: Investigation of the Hierarchical Structure of Kinetic Models in Ignition Problems. Journal Physics of Chemistry **223**, 461–479 (2009)
25. Bykov, V., Maas, U.: Problem adapted reduced models based on Reaction-Diffusion Manifolds (REDIMs). Proc. Combust. Inst. **32**(1), 561–568 (2009)
26. Bykov, V., Maas, U.: The extension of the ILDM concept to reaction-diffusion manifolds. Combust. Theory Model. **11**(6), 839–862 (2007)
27. Bykov, V., Goldfarb, I., Gol'dshtein, V., Greenberg, J.B.: Auto-ignition of a polydisperse fuel spray. Proc. Combust. Inst. **31**(2), 2257–2264 (2007)